Introduction to Computational Neuroscience

Biol 698
Math 635
Biol498
Math 430

Syllabus

Recommended books:

- *Mathematical Foundations of Neuroscience*, by G. B. Ermentrout & D. H. Terman - Springer (2010), 1st edition. ISBN 978-0-387-87707-5

- *Foundations of Cellular Neurophysiology*, by Daniel Johnston and Samuel M.-S. Wu. The MIT Press, 1995. ISBN 0-262-10053-3

- *Dynamical Systems in Neuroscience: The Geometry of Excitability and Bursting*, by E. M. Izhikevich. The MIT Press, 2007. ISBN 0-262-09043-8

- *Biophysics of Computation* - Information processing in single neurons", by C. Koch. Oxford University Press, 1999. ISBN 0-19-510491-9

- *Theoretical Neuroscience*: *Computational and Mathematical Modeling of Neural Systems*, by P. Dayan and L. F. Abbott. The MIT Press,2001. ISBN 0-262-04199-5

Bursting

☑ Silent phase of near-steady-state resting behavior alternating with an active phase of rapid, spikelike oscillations

- Bursting activity in certain thalamic cells, for example, is implicated in the generation of sleep rhythms
- Patients with parkinsonian tremor exhibit increased bursting activity in neurons within the basal ganglia.
- Cells involved in the generation of respiratory rhythms within the pre-Botzinger complex also display bursting oscillations

Bursting

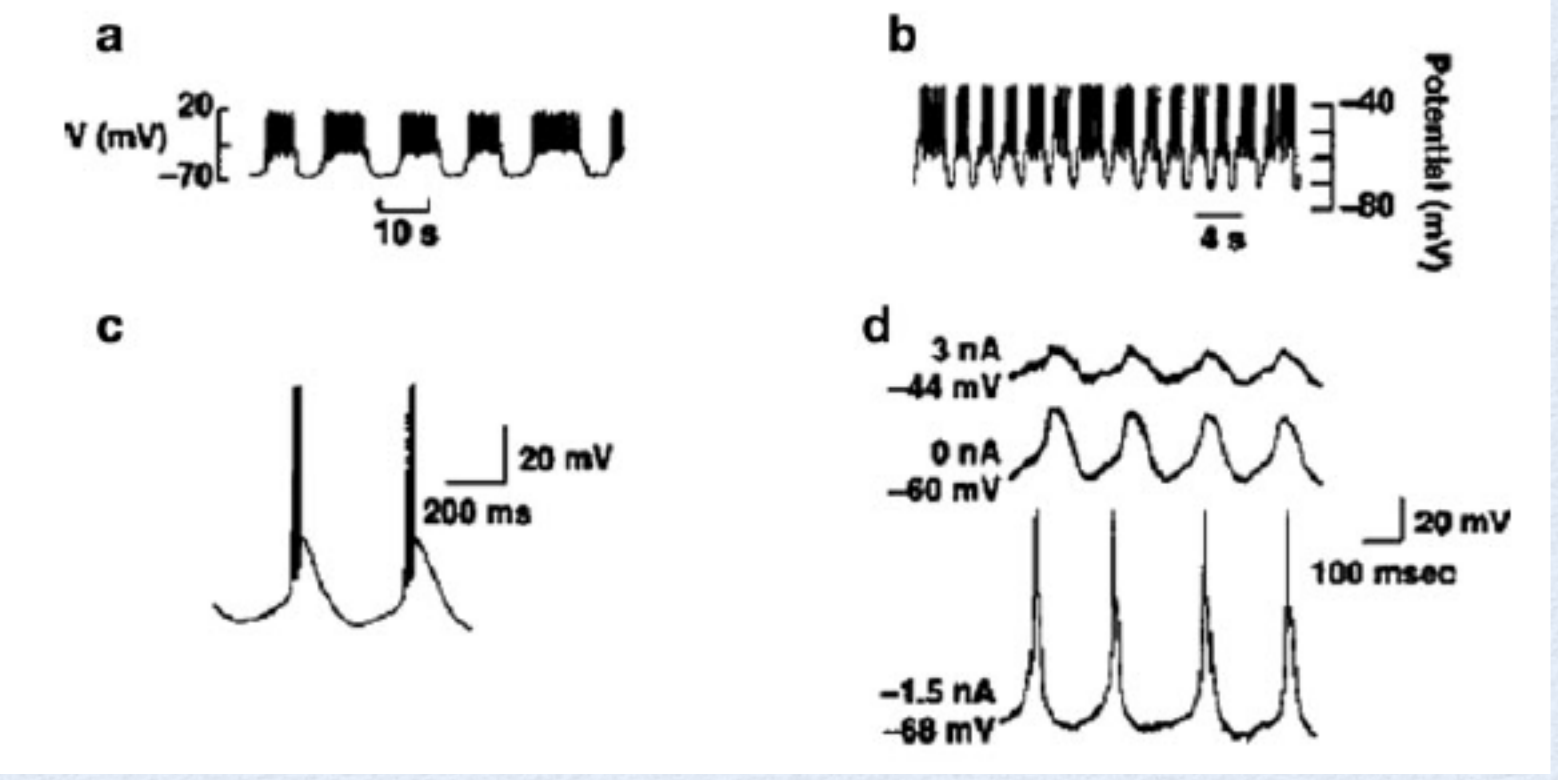

Wang & Rinzel (1995)

Bursting

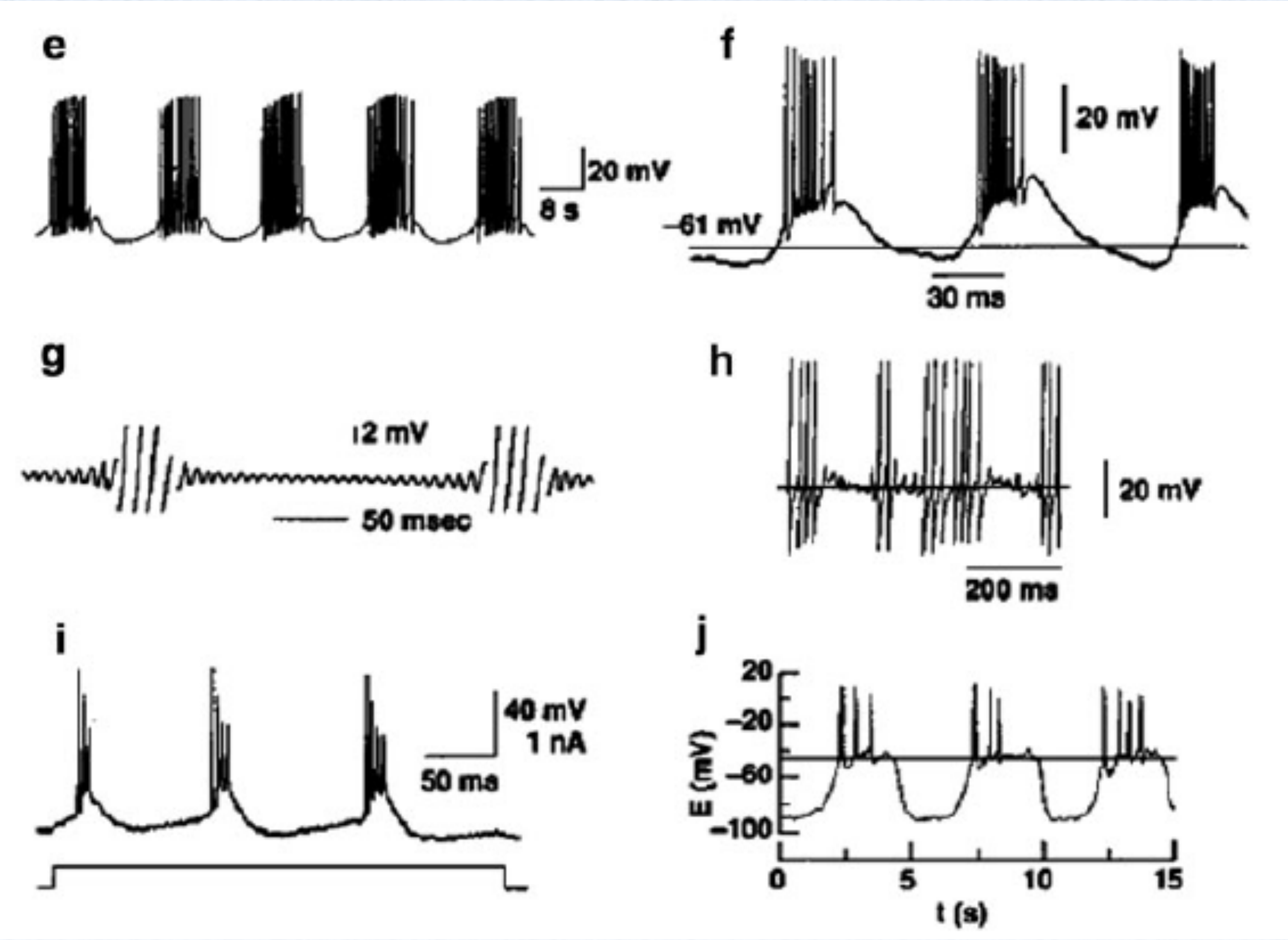

Wang & Rinzel (1995)

Bursting

- ☑ Spiking mechanism (I_{Na}, I_K)
- ☑ Slow modulation: switch between the active and silent phases

Example: I_{KCa} (calcium-dependent potassium)

- Ca^{2+} enters the cell during the active phase
- Activation of I_{KCa} (outward)
- Once I_{KCa} is to large, the cell can no longer sustain spiking activity
- Active phase terminates
- During the silent phase, Ca^{2+} leaves the cell
- Calcium-dependent potassium channels close
- I_{KCa} decreases
- Once I_{KCa} is sufficiently small, spiking resumes

An outward current slowly activates, because of the buildup of Ca^{2+}, and this eventually terminates the spiking phase

Bursting

- ☑ Spiking mechanism (I_{Na}, I_K)
- ☑ Slow modulation: switch between the active and silent phases

Example: I_{Nap} (persistent sodium)

An inward current slowly inactivates, thereby weakening spiking activity

Bursting

- ☑ Square-wave bursters: 3D system (2 fast / 1 slow) - bistability
- ☑ Elliptic bursters: 3D system (2 fast / 1 slow) - bistability
- ☑ Parabolic bursters: 3D systems (1 fast / 2 slow, 2 fast / 2 slow)

Square-wave bursters

- ☑ Pancreatic β cells
- ☑ respiratory generating neurons within the pre-Botzinger complex

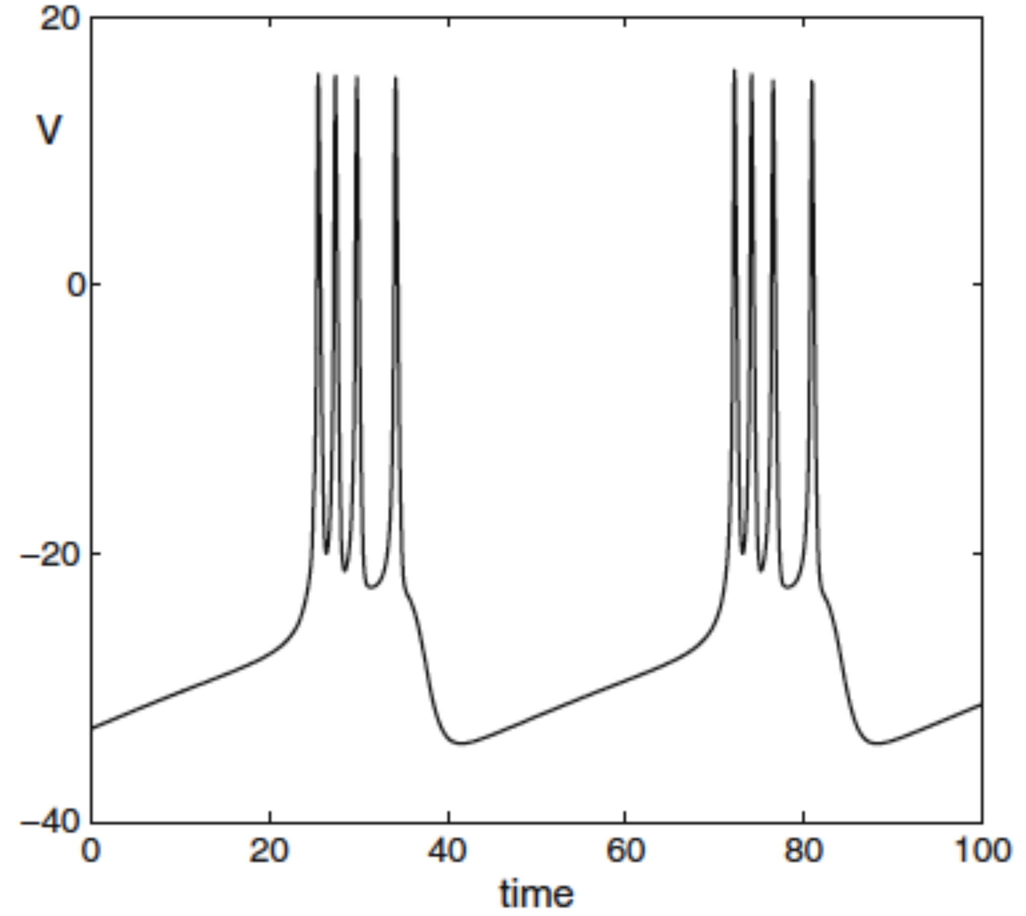

Fig. 5.2 Square-wave bursting. Note that the active phase of repetitive firing is at membrane potentials more depolarized than during the silent phase. Moreover, the frequency of spiking slows down at the end of the active phase

Square-wave bursters

- Morris-Lecar model

$$C_M \frac{dV}{dt} = I_{app} - g_L(V - E_L) - g_K n(V - E_K),$$
$$-g_{Ca} m_\infty(V)(V - E_{Ca}) \equiv I_{app} - I_{ion}(V, n),$$
$$\frac{dn}{dt} = \phi(n_\infty(V) - n)/\tau_n(V),$$

$$m_\infty(V) = \frac{1}{2}[1 + \tanh((V - V_1)/V_2)],$$
$$\tau_n(V) = 1/\cosh((V - V_3)/(2V_4)),$$
$$n_\infty(V) = \frac{1}{2}[1 + \tanh((V - V_3)/V_4)].$$

Table 3.1 Morris–Lecar parameters; the current, I_{app}, is a parameter

Parameter	Hopf	SNLC	Homoclinic
ϕ	0.04	0.067	0.23
g_{Ca}	4.4	4	4
V_3	2	12	12
V_4	30	17.4	17.4
E_{Ca}	120	120	120
E_K	−84	−84	−84
E_L	−60	−60	−60
g_K	8	8	8
g_L	2	2	2
V_1	−1.2	−1.2	−1.2
V_2	18	18	18
C_M	20	20	20

SNLC saddle–node on a limit cycle

Square-wave bursters

- Morris-Lecar model

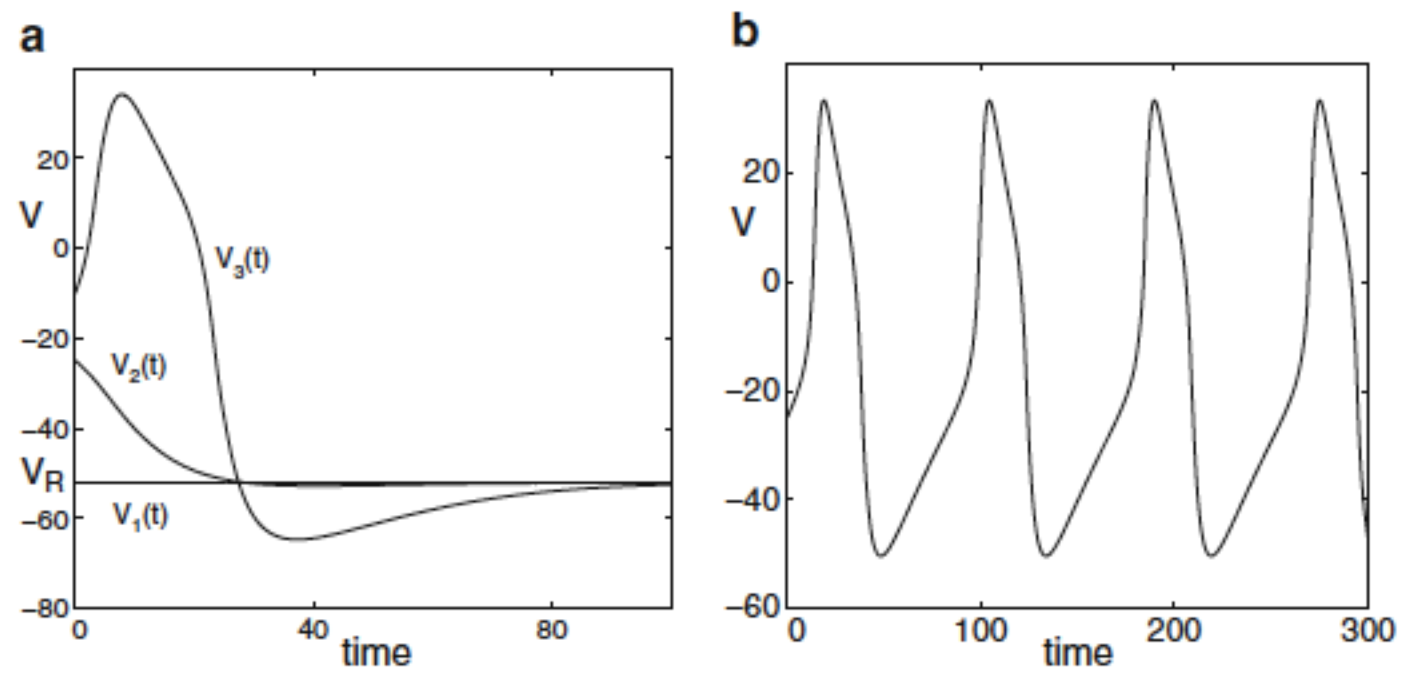

Fig. 3.1 Solutions of the Morris–Lecar equations. Parameters are listed in Table 3.1, the Hopf case. (**a**) A small perturbation from rest decays to the resting state, whereas a larger perturbation generates an action potential. Here, $I_{app} = 60$. (**b**) A periodic solution of the Morris–Lecar equations. Here, $I_{app} = 100$

Square-wave bursters

- Morris-Lecar model

$$C_M \frac{dV}{dt} = -g_L(V - E_L) - g_K n(V - E_K) - g_{Ca} m_\infty(V)(V - E_{Ca}) - I_{KCa} + I_{app},$$

$$\frac{dn}{dt} = \phi(n_\infty(V) - n)/\tau_n(V),$$

$$\frac{d[Ca]}{dt} = \epsilon(-\mu I_{Ca} - k_{Ca}[Ca]),$$

$$I_{KCa} = g_{KCa} z(V - E_K)$$

$$z = \frac{[Ca]^p}{[Ca]^p + 1}$$

Parameter	Square wave	Elliptic	Parabolic
V_1	-1.2	-1.2	-1.2
V_2	18	18	18
V_3	12	2	12
V_4	17.4	30	17.4
E_{Ca}	120	120	120
E_K	-84	-84	-84
E_L	-60	-60	-60
g_K	8	8	8
g_L	2	2	2
g_{Ca}	4	4.4	4
g_{KCa}	0.75	1	1
C_m	1	1	1
I_{app}	45	120	65
ϕ	4.6	0.8	1.33
ϵ	0.1	0.04	0.01
k_{Ca}	1	1	1
μ	0.02	0.01667	0.025
τ_s, g_{CaS}			0.05, 1

Square-wave bursters

- Morris-Lecar model

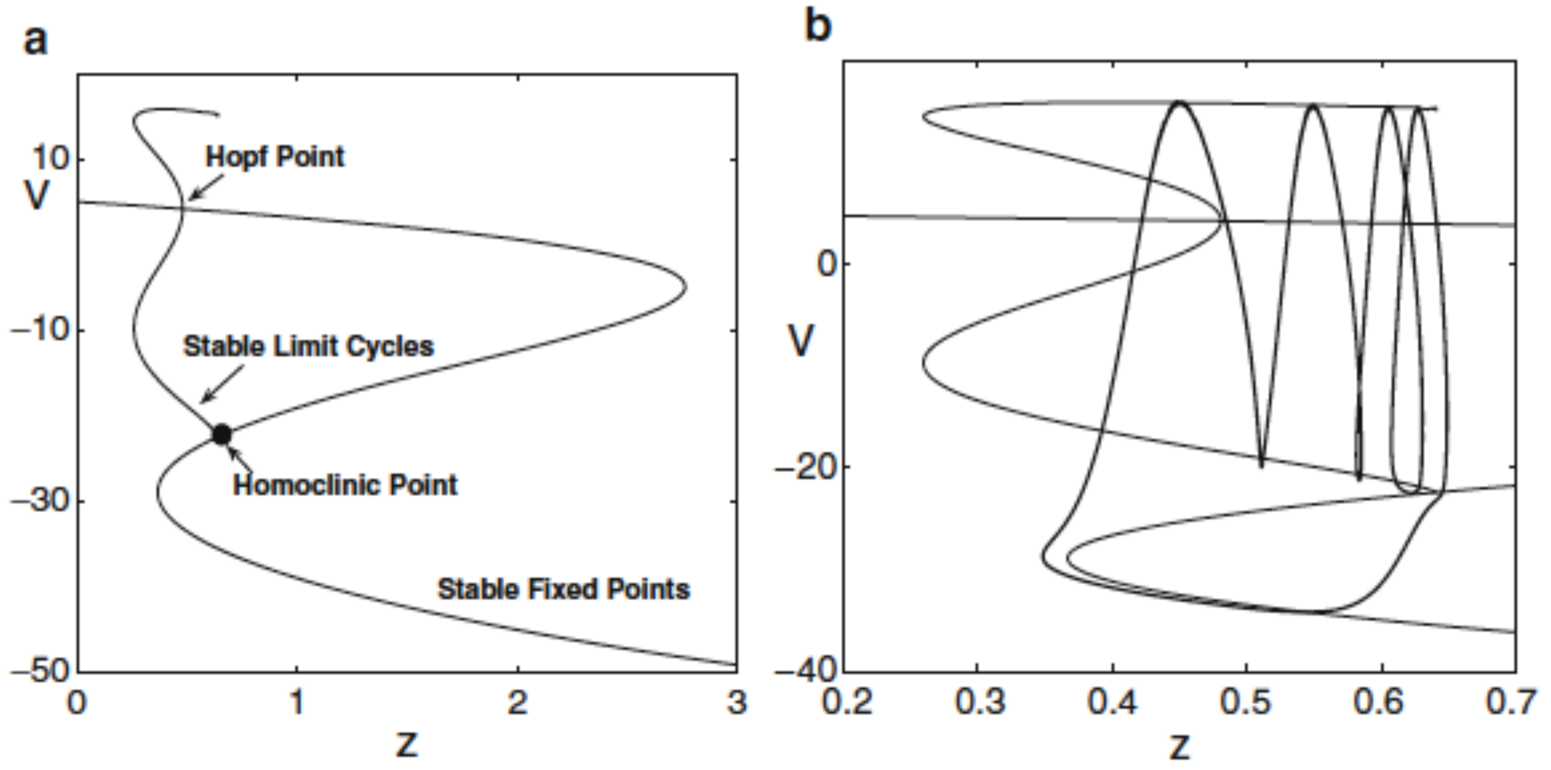

Fig. 5.4 (**a**) Bifurcation diagram of the fast subsystem for square-wave bursters. (**b**) The projection of the bursting trajectory onto the bifurcation diagram

Elliptic & parabolic bursters

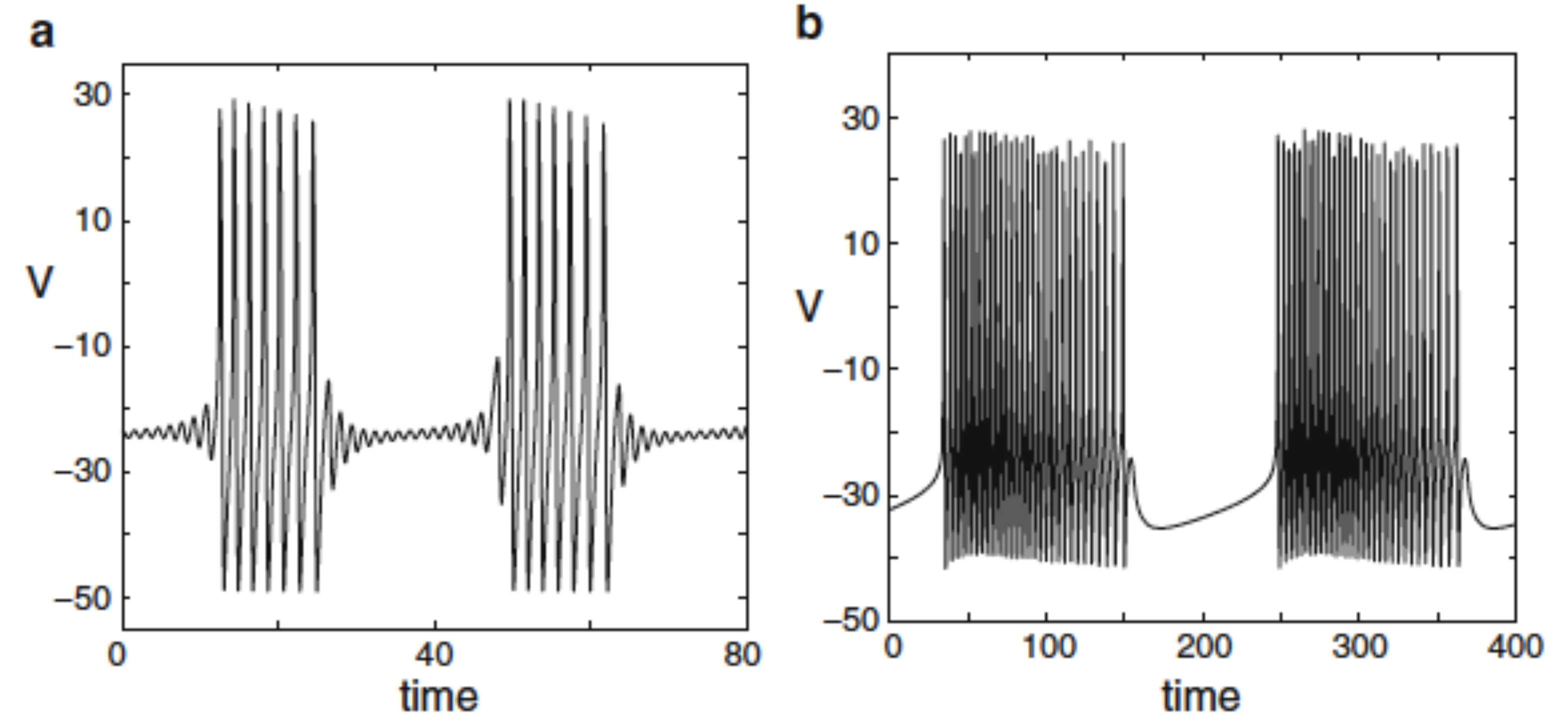

Fig. 5.6 (**a**) Elliptic burster. Note the subthreshold oscillations. (**b**) Parabolic bursting. The frequency of spiking first increases and then decreases during the active phase

Elliptic bursters

- thalamic neurons
- rodent trigeminal neurons
- neurons within the basal ganglia

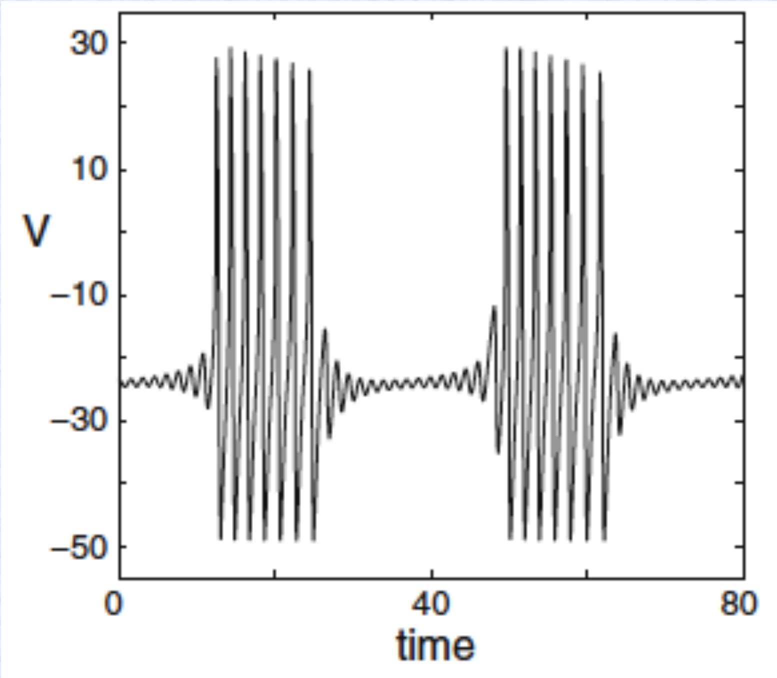

Elliptic bursters

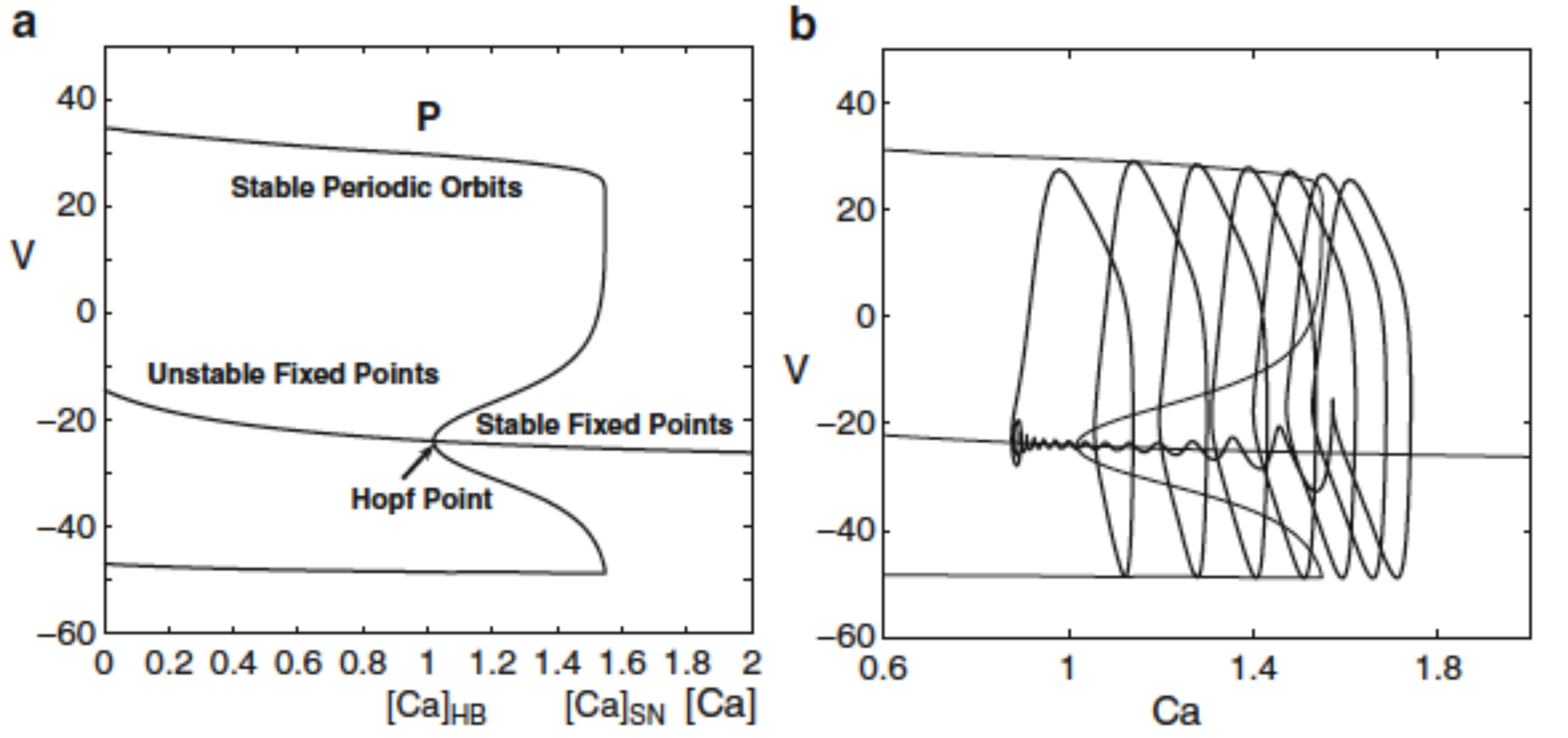

Fig. 5.7 (**a**) Bifurcation diagram associated with elliptic bursting. The projection of the elliptic bursting trajectory onto the bifurcation diagram is shown in (**b**)

Parabolic bursters

- models for Aplysia R-15 neurons

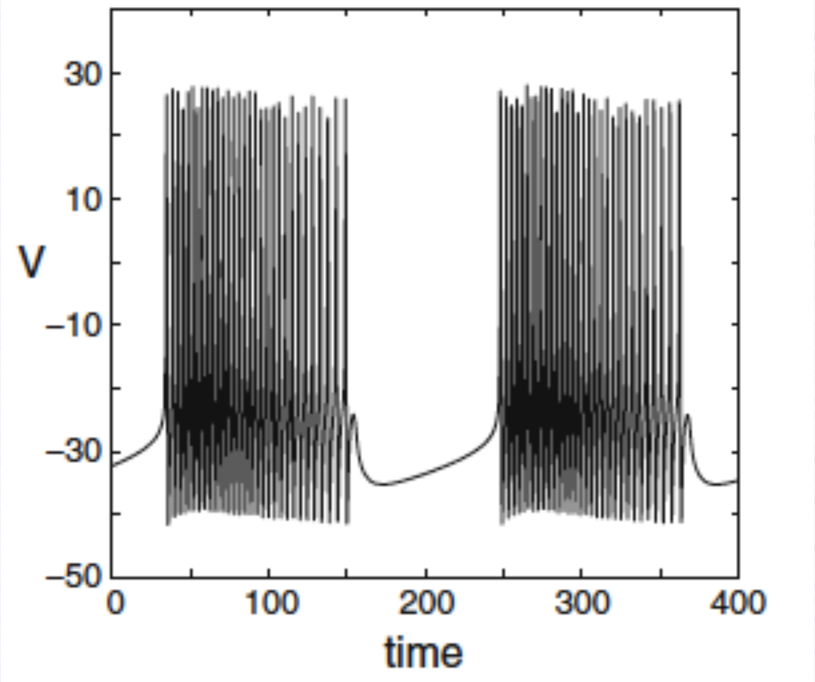

Parabolic bursters

$$
\begin{aligned}
C_{\mathrm{m}}\frac{\mathrm{d}V}{\mathrm{d}t} &= -I_{\mathrm{L}} - I_{\mathrm{K}} - I_{\mathrm{Ca}} - I_{\mathrm{KCa}} - I_{\mathrm{CaS}} + I_{\mathrm{app}},\\
\frac{\mathrm{d}n}{\mathrm{d}t} &= \phi(n_{\infty}(V) - n)/\tau_n(V),\\
\frac{\mathrm{d}[\mathrm{Ca}]}{\mathrm{d}t} &= \epsilon(\mu I_{\mathrm{Ca}} - [\mathrm{Ca}]),\\
\frac{\mathrm{d}s}{\mathrm{d}t} &= \epsilon(s_{\infty}(V) - s)/\tau_s,
\end{aligned}
$$

$$
\begin{aligned}
C_{\mathrm{M}}\frac{\mathrm{d}V}{\mathrm{d}t} &= -g_{\mathrm{L}}(V - E_{\mathrm{L}}) - g_{\mathrm{K}}n(V - E_{\mathrm{K}})\\
&\quad - g_{\mathrm{Ca}}m_{\infty}(V)(V - E_{\mathrm{Ca}}) - I_{\mathrm{KCa}} + I_{\mathrm{app}},\\
\frac{\mathrm{d}n}{\mathrm{d}t} &= \phi(n_{\infty}(V) - n)/\tau_n(V),\\
\frac{\mathrm{d}[\mathrm{Ca}]}{\mathrm{d}t} &= \epsilon(-\mu I_{\mathrm{Ca}} - k_{\mathrm{Ca}}[\mathrm{Ca}]),
\end{aligned}
$$

$$I_{\mathrm{KCa}} = g_{\mathrm{KCa}}z(V - E_{\mathrm{K}})$$

$$z = \frac{[\mathrm{Ca}]^p}{[\mathrm{Ca}]^p + 1}$$

$$I_{\mathrm{CaS}} = g_{\mathrm{CaS}}s(V - E_{\mathrm{Ca}})$$

$$s_{\infty}(V) = 0.5(1 + \tanh(V - 12)/24)$$

Parabolic bursters

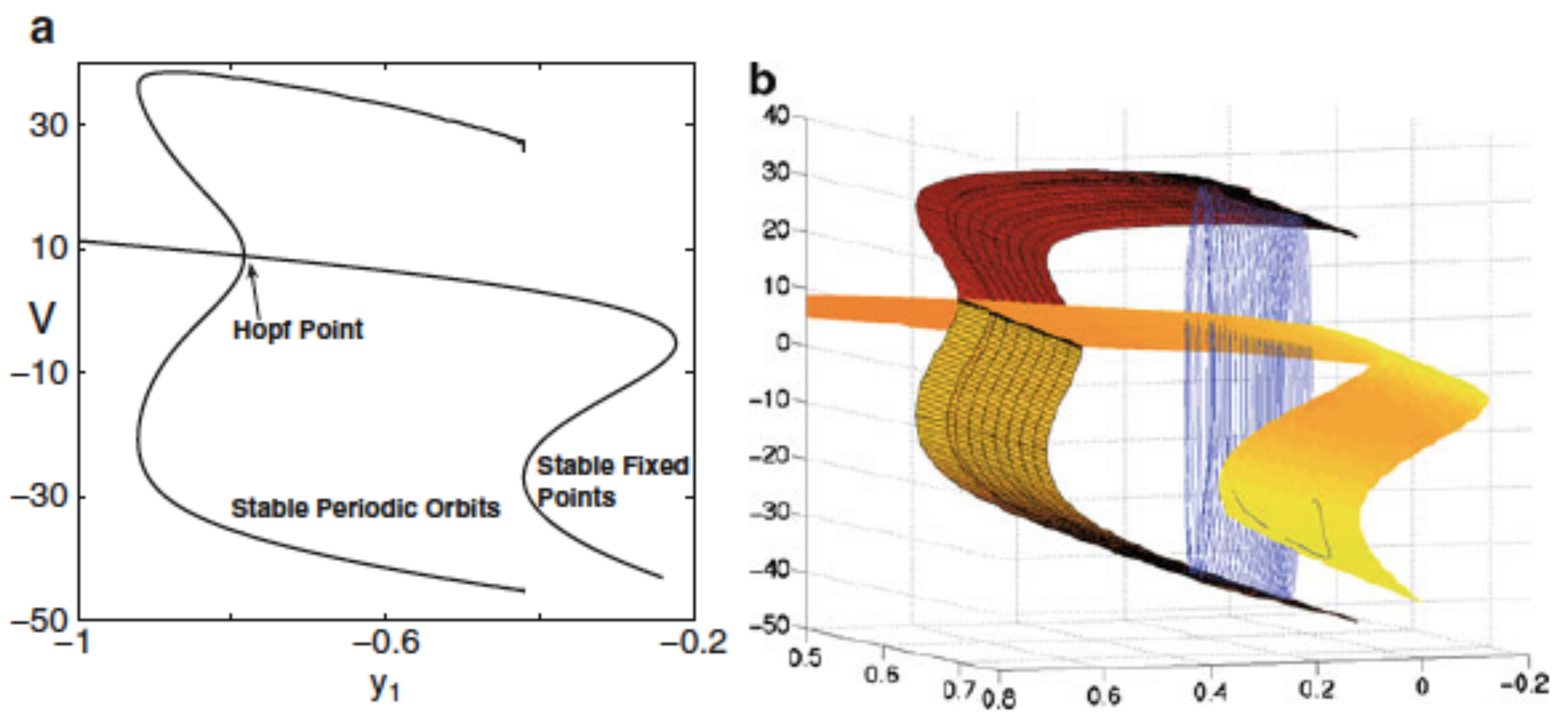

Fig. 5.8 Bifurcation diagram of the fast subsystem for parabolic bursting. (**a**) One of the slow variables is fixed. Note that the branch of periodic orbits ends at a saddle–node on an invariant circle (SNIC). (**b**) With both slow variables as bifurcation parameters, the sets of fixed points and limit cycles form surfaces. Also shown is the projection of the bursting trajectory onto the bifurcation diagram

Parabolic bursters

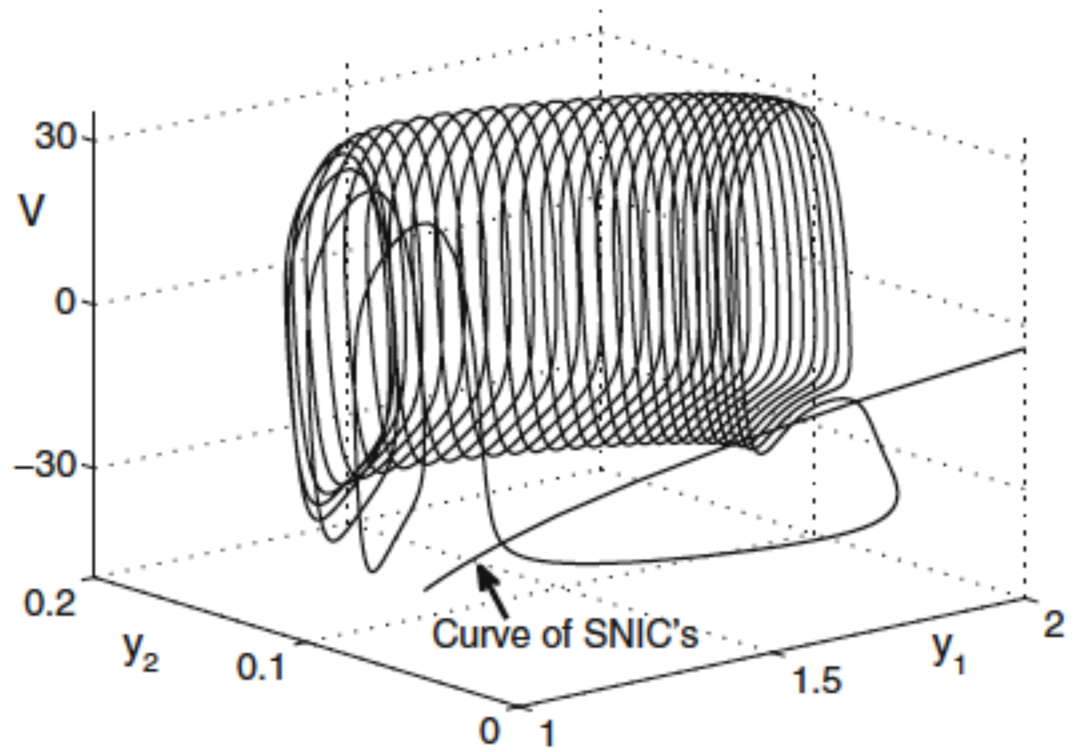

Fig. 5.9 Projection of the parabolic bursting solution onto (V, y_1, y_2)-space. There is a curve in the slow (y_1, y_2)-plane corresponding to SNICs. This curve separates the regions where the fast subsystem exhibits spiking and resting behavior